

All-Fiber Faraday Rotator Made by a Multiturn Figure-of-Eight Coil with Matched Birefringence

V. Annovazzi-Lodi, *Member, IEEE*, S. Donati, *Member, IEEE*, S. Merlo, and A. Leona

Abstract—With a figure-of-eight winding of monomode fiber, we have been able to build multiturn (>100) coils which can be easily trimmed to match the condition of exactly one wavelength-per-turn birefringence. As an example, we report a 45° Faraday rotator intended for an all-fiber optical isolator at $\lambda = 1300$ nm.

I. INTRODUCTION

THE FARADAY rotator is a well-known building block for the realization of several passive components used in optical communications and sensing, such as optical isolators, circulators, Faraday mirrors, and current/magnetic field sensors [1]–[9]. Though the microoptics rotator built around a YIG crystal is well developed and has good performances, considerable interest is attracted by the all-fiber version because of low insertion loss, easier assembly, and not last, feasibility in those spectral ranges where magneto-optical crystals are not available or have excessive transmission loss.

A challenge for the all-fiber version comes from the low value of the Verdet constant V in silica fibers (e.g., $V = 1 \mu\text{rad/A}$ at $\lambda = 1300$ nm as opposed to 2 mrad/A for YIG). Since the Faraday rotation Φ is given by

$$\Phi = V \int_L H \cdot dl \quad (1)$$

it turns out that a considerable length L of fiber (several meters) must be used to get a large rotation (e.g., $\Phi = 45^\circ$ to build an isolator), at reasonable values of H (a few thousands of gauss).

A way to fit the required fiber sample in a small magnet gap, and to build a compact device, is obviously that of winding several turns N on a small (e.g., $R \approx 1$ cm) coil, but in this case the line integral of (1) would give $\Phi = 0$.

Fortunately, as the fiber is bent in the winding, a linear birefringence is superposed to the Faraday rotation, and there exists a matching condition [1]–[4] under which the rotation Φ no longer vanishes. Specifically, if the linear birefringence β_l is equal to $1/R$ (a condition also called wavelength-per-turn matching), then the coil behaves as a pure non reciprocal rotator. The rotation angle Φ is just halved with respect to the value expected for a straight fiber of the same length

$L = 2\pi RN$ [2], [3] and amounts to

$$\Phi = \frac{VHL}{2} = VH\pi RN. \quad (2)$$

A practical limitation [4], [6], [7] for large N is set by the cumulative effect of the small residual error $\epsilon = \beta_l - 1/R$ in the matching of each turn. As N is increased, the tolerable error ϵ is decreased and the required tight mechanical and optical tolerances are increasingly difficult to meet.

Another issue is about the unusually small value of the matching radius that can follow from the condition $R = 1/\beta_l$. For many fibers, and in particular for the standard telecommunication (SM or SMR) fibers, R is less than 3 mm for $\lambda = 1250$ – 1550 nm. Thus, a matched coil would not be feasible at those wavelengths because of excessive curvature loss and increased failure rate by bending.

To circumvent these difficulties, we have devised the figure-of-eight geometry presented in this paper. This design allows us to double the matching radius, thus avoiding curvature losses and fiber breakage, however, it is compact enough to build a rotator based on permanent magnets, and its sensitivity is not much different from the round coil geometry. As an example of application, we report on an isolator we have developed for optical communication in the second window ($\lambda \approx 1300$ nm).

II. THE FARADAY ROTATOR

The proposed geometry has been schematized in Fig. 1(a) and (b), where two different options for the input/output fiber have been considered. The bend radius is selected so that each half turn of the figure-of-eight is a half-wave retarder; this allows Faraday contributions of opposite sign, arising on opposite sides of the coil, to be cumulated, much as in the basic round coil geometry [2], [3], [7].

In order to get a rotator, we have found two possible arrangements of the coil with respect to the magnetic field: 1) the figure-of-eight can be laid along the direction of the magnetic field [Fig. 1(c)] and then we need a uniform field and the input/output fibers must be placed in the middle as in Fig. 1(a); or 2) the figure-of-eight can be laid orthogonal to the magnetic field [Fig. 1(d)], and then two magnets with opposite polarities are required and the input/output fibers must be placed on one side as in Fig. 1(b).

To analyze the rotation under a magnetic field, we have used the Jones formalism following the method presented in [6]. Under the small perturbation approximation $VH \ll 1/\beta_l$, the differential equation for the evolution of the Jones vector

Manuscript received March 14, 1995; revised September 15, 1995. This work was supported in part by the CNR (Progetto Finalizzato MADESS) and SIRT SpA, Milan, Italy. The work of A. Leona was supported by a scholarship from SIRT SpA.

The authors are with the Department of Electronics, University of Pavia, Pavia, Italy.

IEEE Log Number 9415874.

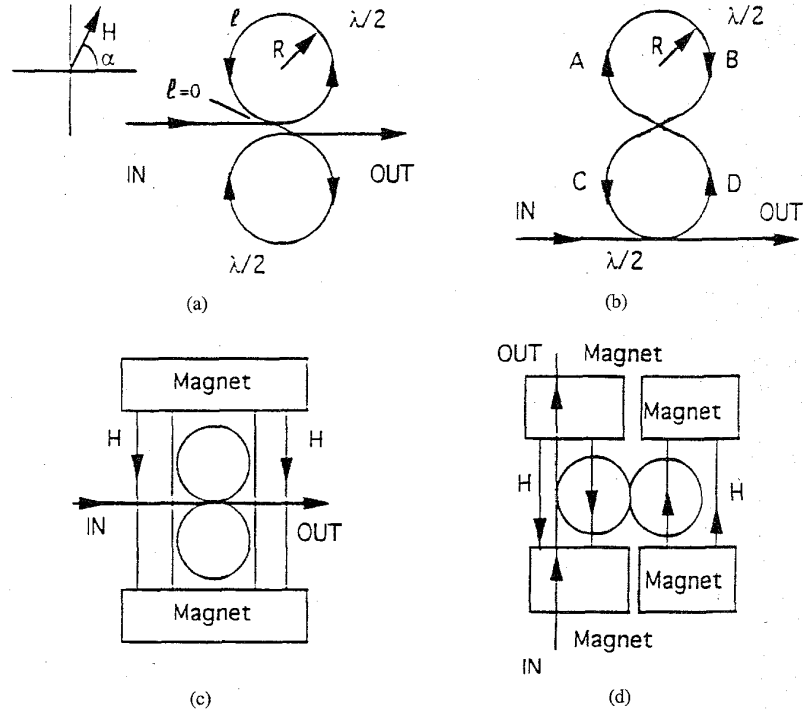


Fig. 1. Figure-of-eight matched coil in a uniform magnetic field H with two input/output schemes (a), (b). Each half turn is a half wave retarder so that Faraday rotation is cumulated on a complete turn. Experimental arrangements for building an all-fiber Faraday rotator are shown in (c), (d).

$\vec{E}(\ell)$ along the coil has been solved, looking for a solution in terms of superposition of the bending birefringence effect and of a small contribution \vec{e}_o due to the Faraday effect, i.e.,

$$\vec{E}(\ell) = \begin{bmatrix} E_x \\ E_y \end{bmatrix} = \begin{bmatrix} e^{i(\beta_1 \cdot \ell/2)} & 0 \\ 0 & e^{-i(\beta_1 \cdot \ell/2)} \end{bmatrix} \vec{E}_i + \vec{e}_o \quad (3)$$

where $\vec{E}_i = \vec{E}(0)$ is the Jones vector of the input field. Letting $\beta_1 = 1/2R$, we obtain two linear differential equations for the components of \vec{e}_o which are integrated in polar coordinates [6]; with the proper initial conditions, we find the following expressions for the output field components at $\ell = 4\pi R$, i.e., after one full turn of the figure-of-eight coil of Fig. 1(a):

$$E_x = E_{ix} + 2HVE_{iy} \left(\frac{e^{i\alpha}}{2R} - \frac{e^{-i\alpha}}{3i} \right) \quad (4a)$$

$$E_y = E_{iy} - 2HVE_{ix} \left(\frac{e^{i\alpha}}{3i} - \frac{e^{-i\alpha}}{2R} \right) \quad (4b)$$

where α is the angle between the magnetic field and the minor axis of the coil. From (4a) and (4b), a condition must be satisfied to obtain a pure nonreciprocal rotation: for a linear input polarization at an arbitrary angle, both terms in brackets in (4a) and (4b) must be real, hence, we have $\alpha = \pi/2$, i.e., the magnetic field and the wavevector at the input have to be orthogonal as in the layout of Fig. 1(c).

For a coil of N complete turns the rotation is then found to be:

$$\Phi = \left(\frac{16}{3} \right) NHVR \quad (5)$$

and comparing (5) to (2) we can see that there is only a minor decrease (a factor 0.83) with respect to the round coil geometry of the same length.

Instead, for the geometry of Fig. 1(b), a pure rotation is obtained by taking $\alpha = 0$, provided that H has opposite direction on odd and even half-turns of the figure-of-eight [Fig. 1(d)]. With this assumption the rotation is calculated as

$$\Phi = \left(\frac{8}{3} \right) NHVR. \quad (6)$$

If the magnetic field is applied only on the top and bottom quarters [i.e., arcs AB, CD in Fig. 1(b)] of the coil, we get a somewhat higher rotation, i.e.,

$$\Phi = \left(\frac{8\sqrt{2}}{3} \right) NHVR. \quad (7)$$

This configuration is interesting for a Faraday rotator because the magnet gap is halved, i.e., H is increased or the magnet size can be reduced; however, it is not suitable for a sensor of (uniform) magnetic field.

The above analysis has been derived under the assumption of small perturbations; however, we have found numerically that (5)–(7) are a good approximation even when the reciprocal birefringence and the Faraday effect are comparable.

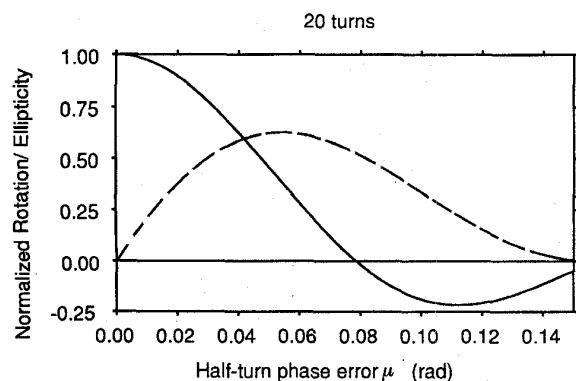


Fig. 2. Normalized rotation angle (full line) and ellipticity (dotted line) at the output of a figure-of-eight coil for $\alpha = \pi/2$ and $N = 20$ turns as a function of half-turn retardation error μ .

III. TRIMMING ERRORS

Let us now evaluate the effect of trimming errors around the birefringence matching condition $\beta_l = 1/2R$, of importance especially for the long coils ($N > 100$). First, let us assume a constant birefringence mismatch $\varepsilon = \beta_l - 1/2R$ (per turn) on all the turns, due for example to a systematic error on the former or on the fiber outer radius.

Taking $\varepsilon \ll 1/2R$, and carrying out the analysis as in [6] for $\alpha = \pi/2$ [Fig. 1(a) and (c)], we find for the rotation Φ :

$$\Phi = \left(\frac{16}{3}\right)NHVR \operatorname{sinc}(2N\mu) \quad (8)$$

where $\mu = 2\pi R\varepsilon$ is the phase error on each half turn and the term $\operatorname{sinc}(2N\mu)$ gives the decrease of the Faraday rotation due to mismatch. Also, for $\varepsilon \neq 0$ it is found that the output field is not linearly polarized and its ellipticity depends on μ . These results are shown in Fig. 2 for $N = 20$.

Because of the cumulative effect of trimming errors, there is a maximum number of turns $N \approx 1/2\mu$ which is usable without incurring into a substantial decrease of rotation. This impacts on the precision of R ; for example, to have a decrease $< 10\%$ in a coil with $N = 75$ turns, the geometrical tolerances of the former and of fiber coating diameter must be within $1 \mu\text{m}$, a value next to that found for the round coil geometry [6].

A suitable trimming method must therefore be envisaged. In a previous paper, a piezoelectric former [2] was used for the round coil to apply [10], [12] tension birefringence through small variations of R , but an electrical actuation is objectionable in sensing applications as well as in isolators for optical communications.

We have found that with the figure-of-eight geometry the systematic error is easily zeroed by trimming the distance of the two cylindrical formers. This method has two main effects [10]–[12]: 1) change in the strain-induced birefringence due to mechanical tension, and 2) change in the length of fiber laying on the former and subjected to bending birefringence. (A third effect, i.e., the change in bend radius due to coating compression has been evaluated as negligible.)

With reference to Fig. 3, let $2D$ be the former distance when the coil is wound while $2(D+d)$ is the distance after trimming.

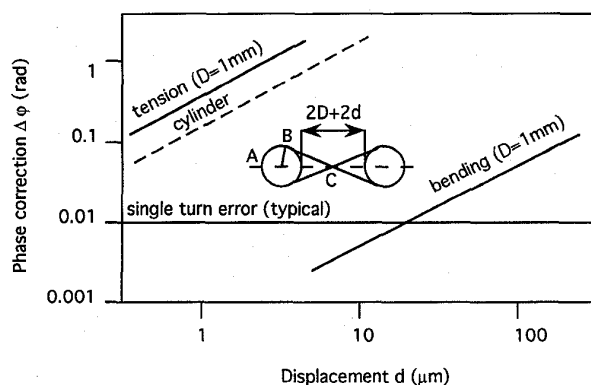


Fig. 3. Trimming diagram of a figure-of-eight coil ($R = 5$ mm) showing the phase correction per turn $\Delta\varphi$ obtained by increasing the gap from $D = 1$ mm to $D + d$. A typical single-turn error (due to a radius mismatch $\Delta R = 10 \mu\text{m}$) is also shown. The phase correction for a cylindrical coil (dotted line) is reported for comparison.

The fiber length of a single turn laying on the former is

$$S = 4AB = 4R \left[\frac{\pi}{2} + \arcsin \left(\frac{R}{R+D} \right) \right] \quad (9)$$

for $d = 0$, and varies as the tangential point B moves when distance is increased. The total length of a single turn ($d = 0$) is thus:

$$L = S + 4(D^2 + 2DR)^{1/2}. \quad (10)$$

From (10), we can now calculate the fiber strain $\Delta L/L = [L(D) - L(D+d)]/L(D)$ and get the phase correction $\Delta\varphi$ from the well-known expressions [11]. In Fig. 3 we plot $\Delta\varphi$ as a function of d ranging from 1 – $100 \mu\text{m}$ for $D = 1$ mm, along with the typical single turn phase error calculated for a radius mismatch $\Delta R = 10 \mu\text{m}$.

From these data it would appear that the strong effect of tension on $\Delta\varphi$ calls for a very fine resolution on d ; however, an effective buffering action between the fiber and the former is supplied by the primary coating. Since the Young modulus of silica is about 20–100 times larger than that of most plastic polymers [13], there is a substantial reduction of fiber stress at a given d . In practice, the correction of a typical one-turn error (0.01 rad) is obtained experimentally by varying d in the range 1 – $10 \mu\text{m}$.

The length variation $\Delta S(d)$ due to a change of the former distance d is found from (9), and from this result one can calculate the single turn phase correction $\Delta\varphi$ which is also reported in Fig. 3 (bending), just a minor effect with respect to tension.

The above results assume a coil with the fiber ends blocked. However, if the fiber is allowed to slide, trimming can be performed mainly by bending birefringence and the resolution on d is significantly relaxed. Usually, in a coil with large N , friction prevents the fiber from sliding onto the former. Nevertheless, a substantial change of the initial birefringence can be obtained simply by loosening the coil and restarting with a different D . In this way, the tension of the figure-of-eight can be always kept low.

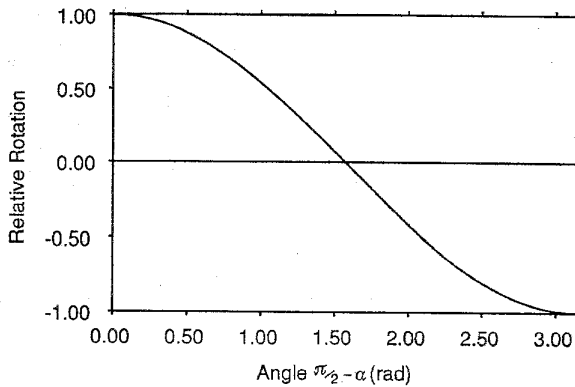


Fig. 4. Normalized rotation angle for a figure-of-eight coil as a function of the orientation of the magnetic field.

Mechanical trimming can be implemented also with the round coil geometry, by cutting in halves the former and introducing an actuator between them. Fig. 3 shows that for $R = 5$ mm the correction $\Delta\varphi$, due to tension, for the round coil is comparable to that of the figure-of-eight. Nevertheless, in the first case trimming can be achieved only by tension, and if too large a value is reached, one should remake the former with a different radius.

After systematic errors have been removed, a small random error ε_i is left on each turn, due to localized birefringence fluctuations. By numerical analysis we have found that if ε_i is small on the single turn ($4\pi\varepsilon_i \ll 1/R$), is statistically uniform on the coil and has zero average, then the total rotation reduction does not exceed that due to the worst turn, i.e., $\text{sinc}[4\pi R \max(\varepsilon_i)]$. A similar result has been reported for the cylindrical coil [7].

Therefore, the diagram of Fig. 2, which was derived for a 20 turn figure-of-eight coil, can still be used entering $\mu = 4\pi R \max(\varepsilon_i)/20$ on the abscissa to adjust the scale factor.

As a function of wavelength, the matching condition is met in an interval becoming narrower as N is increasing. This effect can also be used to make a filter, but we will not discuss this topic here. When the coil is trimmed at a given wavelength λ , the error ε at $\lambda' = \lambda + \Delta\lambda$ is easily calculated as $\varepsilon = \Delta\lambda/2\pi\lambda R$, since β_l is proportional to $1/R\lambda$. Therefore, the decrease of rotation is still described by Fig. 2, by using $\mu = 2\pi R\varepsilon = \Delta\lambda/\lambda$ on the x -axis. The allowable optical bandwidth $\Delta\lambda$, for a maximum rotation reduction of 10% in a coil of $N = 80$ turns, is of about 1.2 nm at $\lambda = 1300$ nm.

We have also investigated the effect of a small circular birefringence in the coil, which can arise from unintentional torsion of the fiber during winding. It is well known that a constant circular birefringence β_c is quenched if the condition $\beta_c \ll \beta_l$ holds [14]. Moreover, re-writing (3) to include circular birefringence, it can be shown that on a trimmed coil the effect of β_c vanishes on any integer number of turns.

IV. THE ALL-FIBER ISOLATOR

The Faraday rotator based on the figure-of-eight matched coil has been employed to make an all-fiber isolator for the second window ($\lambda = 1300$ nm). The geometry of Fig. 1(c)

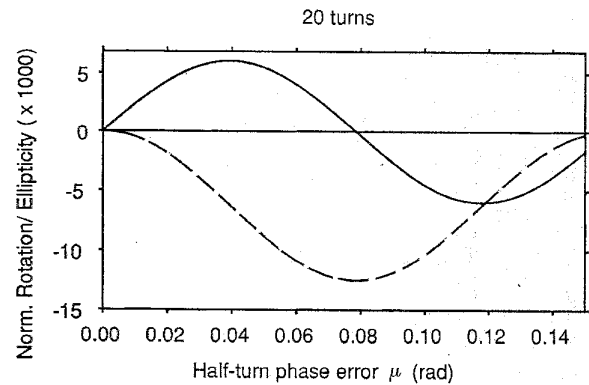


Fig. 5. Normalized rotation angle (full line) and ellipticity (dotted line) at the output of a figure-of-eight coil for $N = 20$ turns for $\alpha = 0$ as a function of the half-turn retardation error.

was preferred because it has the maximum specific rotation and needs a single magnet.

We used commercially available Nd-Fe-B magnets yielding $H = 6$ KG in a 2 cm gap. The fiber was the "oligomodal" Ensign 2300, which has a cutoff wavelength $\lambda_c = 1700$ nm and allows single mode low loss propagation in the second window at the matching radius $R = 5$ mm. From (5), the desired 45° rotation at $\lambda = 1300$ nm requires about 62 turns of fiber. We used $N = 70 - 80$ full figure-of-eight turns and performed functional trimming in two steps. First, by moving the two cylinders away from each other we got a linearly polarized output with a rotation slightly in excess of 45° . A compact mechanical stage with differential micrometer screws was employed to ensure adequate resolution.

Then, the desired 45° rotation was obtained by tilting the coil in the magnet gap. This method allows us to trim rotation without introducing ellipticity, since the matched coil is sensitive only to the magnetic field component parallel to its vertical axis, while the other component affects neither rotation nor ellipticity. This result, which represents a specific advantage of the figure-of-eight, is illustrated in Fig. 4 where the angular sensitivity of the coil has been calculated as a function of the deviation from $\alpha = \pi/2$. Even if $\varepsilon \neq 0$ (unmatched coil), the sensitivity to the orthogonal component of H ($\alpha = 0$) is small, as shown in Fig. 5, and this fact relaxes the requirement on the field uniformity.

All-fiber polarizers were finally spliced at each end of the rotator to build the isolator. Performances of the device, measured with standard laboratory equipment are as follows.

- Isolation loss better than 38 dB at $\lambda = 1320$ nm and better than 30 dB in the range 1318 to 1322 nm as shown in Fig. 6. The isolation at the peak wavelength is limited by the extinction of the polarizers.
- Insertion loss less than 2 dB, mainly due to splices between the rotator and the polarizers (the loss of the rotator alone is less than 0.17 dB).

V. CONCLUSIONS

In conclusion, we have demonstrated that the figure-of-eight geometry is a viable approach for wavelength-per-turn

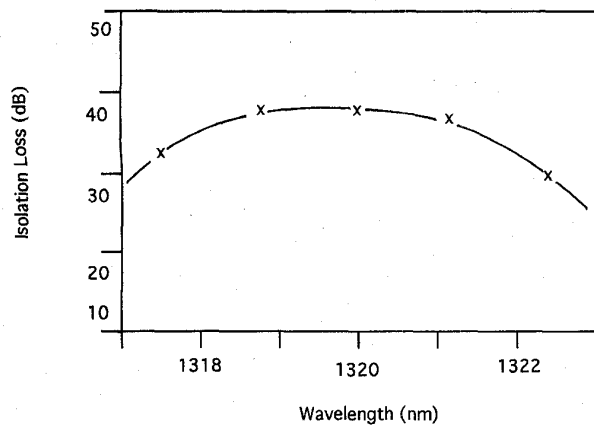


Fig. 6. Isolation loss of the all-fiber optical isolator as a function of wavelength.

matched birefringence Faraday rotators. We have also reported on an all-fiber isolator for $\lambda = 1300$ nm which performs a good isolation and is completely passive as it uses a permanent magnet. The proposed geometry can be useful also for implementing other components such as Faraday mirrors and magnetic field sensors for all-fiber systems, particularly at those wavelengths where magneto-optical crystals like YIG's and related garnets are not available.

REFERENCES

- [1] E. H. Turner and R. H. Stolen, "Fiber Faraday circulator or isolator," *Opt. Lett.*, vol. 6, pp. 322-323, July 1981.
- [2] G. Day, D. N. Payne, A. J. Barlow, and J. J. Ramskov-Hansen, "Faraday rotation in coiled, monomode optical fibers: Isolators, filters, and magnetic sensors," *Opt. Lett.*, vol. 7, pp. 238-240, May 1982.
- [3] V. Annovazzi Lodi and S. Donati, "Combined reciprocal and nonreciprocal birefringence in optical monomode fibers," *Optic. Quantum Electron.*, vol. 15, pp. 381-388, Sept. 1983.
- [4] G. Day, D. N. Payne, A. J. Barlow, and J. J. Ramskov-Hansen, "Design and performance of tuned fiber coil isolators," *J. Lightwave Technol.*, vol. LT-2, pp. 56-60, Feb. 1984.
- [5] S. Donati, V. Annovazzi Lodi, and T. Tambosso, "Magneto-optical fiber sensors for the electrical industry: Analysis of performances," in *IEE Proc.s-J. Optoelectron.*, vol. 135, pp. 372-382, Oct. 1988.
- [6] V. Annovazzi Lodi, S. Donati, and S. Merlo, "Coiled-fiber sensor for vectorial measurement of magnetic field," *J. Lightwave Technol.*, vol. LT-10, pp. 2006-2010, Dec. 1992.
- [7] V. Annovazzi Lodi, S. Donati, S. Merlo, and L. Zucchelli, "Vectorial magnetic-field fiber-optic sensor based on accurate birefringence control," in *Proc. OFS-9*, May 1993, pp. 293-296.
- [8] G. Bendelli and S. Donati, "Optical isolators for telecommunications: Review and current trends," *ETT-European Trans. Telecommun.*, vol. 3, pp. 373-380, July-Aug. 1992.
- [9] N. C. Pistoni and M. Martinelli, "Polarization noise suppression in retracing optical fiber circuits," *Opt. Lett.*, vol. 16, no. 10, pp. 711-713, May 1991.
- [10] S. C. Rashleigh, "Origins and control of polarization effects in single-mode fibers," *J. Lightwave Technol.*, vol. LT-1, pp. 312-331, June 1983.
- [11] S. C. Rashleigh and R. Ulrich, "High birefringence in coiled single mode fibers," *Opt. Lett.*, vol. 5, pp. 354-356, May 1980.
- [12] R. Ulrich, S. C. Rashleigh, and W. Eichhoff, "Bending induced birefringence in single mode fibers," *Opt. Lett.*, vol. 5, pp. 273-275, June 1980.
- [13] D. E. Gray, Ed., *American Institute of Physics Handbook*. New York: McGraw-Hill, 1972, 3rd ed.
- [14] S. C. Rashleigh and R. Ulrich, "Magneto-optic current sensing with birefringent fibers," *Appl. Phys. Lett.*, vol. 21, pp. 768-770, May 1979.

- [15] K. Warbrick, "Single-mode optical isolator at 1.3 μm using all-fiber components," *Electron. Lett.*, vol. 22, no. 13, pp. 711-713, June 1986.



V. Annovazzi-Lodi (M'89) was born in Novara, Italy, on November 7, 1955. He received the degree in electronic engineering from the University of Pavia, Pavia, Italy, in 1979.

Since then he has been working at the Department of Electronics of the University of Pavia in the field of electro-optics. His main research interests include injection modulation phenomena and chaos in lasers, electrical fiber sensors, the fiber gyroscope, passive fiber components for telecommunications and sensing, transmission via diffused infrared radi-

ation. In 1983, he became a staff researcher of the Department of Electronics of the University of Pavia and in 1992 he became an associate professor in the same institution.

Dr. Annovazzi-Lodi is a member of the AEI.



S. Donati (M'75) received the degree in physics from the University of Milan in 1966.

For nine years, he was with CISE (Milan), working on noise in photomultipliers and avalanche photodiodes, nuclear electronics, and electrooptic instrumentation (laser telemetry, speckle pattern interferometry, gated vision in scattering media). In 1975, he joined the Department of Electronics, University of Pavia, as internal lecturer and worked on feedback interferometers, fiber gyroscope, and noise in CCD's. In 1980, he became full professor of optoelectronics, and since then his main research interests have been optical fiber sensors, passive fiber components for telecommunications, free-space and guided optical interconnections, locking, and chaos in lasers. He has authored or coauthored about 100 papers and holds four patents.

Dr. Donati is a member of the AEI, APS, OSA, ISHM, and has actively served to organize several national and international meetings and schools in the steering and program committees or as chairman. He also worked in the standardization activity CEI/IEC (CT-76 laser safety and CT-86 optical fibers).



S. Merlo was born in Pavia, Italy, in 1962. She received the degree in electronic engineering from the University of Pavia in 1987, the M.S.E. degree in bioengineering from the University of Washington, Seattle in 1989, and the Ph.D. degree in electronic engineering and computer science from the University of Pavia in 1992.

Since 1993 she has been faculty member of the Department of Electronics at the University of Pavia. Her research interests include fiber-optic sensors for biochemical and electrical applications, advanced photodetection techniques and all-fiber passive components for telecommunications and sensors, and laser interferometry.



A. Leona was born in Ivrea, Italy, in 1969. He received the degree in electronic engineering from the University of Pavia, Italy in 1994.

His main research interests are in passive fiber-optic components for optical communications.